
Learning Manipulation Skills through Robot Chain-of-Thought with Sparse Failure Guidance

Kaifeng Zhang¹, Zhao-Heng Yin², Weirui Ye^{3,1,4} and Yang Gao^{3,1,4}

¹Shanghai Qi Zhi Institute ²UC Berkeley ³Tsinghua University ⁴Shanghai AI Lab

Abstract

The acquisition of manipulation skills through language instruction remains an unresolved challenge. Recently, vision-language models have made significant progress in teaching robots these skills. However, their performance is restricted to a narrow range of simple tasks. In this paper, we propose that vision-language models can provide a superior source of rewards for agents. Our method decomposes complex tasks into simpler sub-goals, enabling better task comprehension and avoiding potential failures with sparse failure guidance. Empirical evidence demonstrates that our algorithm consistently outperforms baselines such as CLIP, LIV, and RoboCLIP. Specifically, our algorithm achieves a $5.4\times$ higher average success rate compared to the best baseline, RoboCLIP, across a series of manipulation tasks. It has shown a comprehensive understanding of a wide range of robotic manipulation tasks.

1 Introduction

Learning manipulation skills from language instruction is a critical challenge in robot learning. Despite advancements [1, 2, 3], mastering robot manipulation remains an unresolved problem. Recently, vision-language models such as CLIP [4], LIV [5], Flamingo [6], PaLM [7], and GPT-4V have markedly improved robots’ capabilities in acquiring manipulation skills [5, 8, 9]. However, these models are limited to a narrow range of simple tasks, such as closing a drawer. Additionally, CLIP [10] and LIV [5] focus on language and visual goal alignment but lack an understanding of the dynamics of manipulation process. Conversely, RoboCLIP [11] captures the temporal information from robot movements with a video backbone S3D [12], yielding a better understanding of manipulation process. However, RoboCLIP lacks spatial reasoning capabilities and task completion awareness.

By analogy, consider how children learn. They break complex tasks into manageable stages, simplifying the task and facilitating its completion. For instance, to open a door, children decompose the task into sub-goals such as approaching the handle, grasping it, pulling it back, and opening the door. During learning, they also draw lessons from potential failures and successes, guided by parental advice and reinforcement.

Our algorithm draws inspiration from child learning paradigms. To better understand the manipulation task process, we use a robot chain-of-thought to decompose tasks into a series of actionable steps, leveraging prior task knowledge from foundation models. Meanwhile, we provide sparse human failure guidance, highlighting potential failures for the agents. The designed reward mechanism yields higher rewards when the robot performs tasks in line with task descriptions while avoiding potential failure cases. To reinforce the task completion process, we collect success experiences through foundation models to strengthen the policy.

In this paper, we present a novel framework named Rewarder from **Robot Chain-of-Thought** with **Sparse Failure Guidance** (RoboCoT). Our RoboCoT introduces an innovative reward feedback mechanism using vision language foundation models to equip robots with a broad spectrum of

manipulation skills. We demonstrate that our approach performs well across a broad spectrum of tasks, achieving a $5.4\times$ performance improvement over the best existing baseline. Ablation studies show that each component of our algorithm contributes to the overall performance.

2 Related Work

2.1 Learning Manipulation Skills for Robotics

Acquiring general manipulation abilities can be facilitated through learning from expert demonstrations, using behavioral cloning (BC) [13, 14, 15] and inverse reinforcement learning (IRL) [16, 17]. BC directly maps the state space to the action space to mimic the expert’s actions. However, BC faces several limitations, including compounding errors [18], the copycat problem [19], and out-of-distribution sample shifts [20]. In contrast, IRL derives both the reward function and the policy from expert demonstrations. However, IRL struggles with sample efficiency, particularly in real-world applications [21, 22, 23].

Mastering manipulation skills with language inputs directly presents several challenges, such as a lack of reward signals and inefficiency in understanding vision-language contexts. Recent studies have explored integrating foundation models to enhance the understanding of language instructions [24]. Our algorithm is designed to learn manipulation skills from language inputs by effectively leveraging pre-trained vision-language models as a source of rewards.

2.2 Foundation Models for Robotics

Vision-language foundation models equip robot agents with compact pre-trained representations. R3M [25] co-trains video and language instructions in a self-supervised manner [26], enhancing the robot’s ability to mimic expert actions. PaLM-E [9] integrates visual observations with large language models, facilitating low-level robot control that includes reasoning about the control process. RT-1 [1] uses transformers to better mimic expert behaviors. RoboFlamingo [8] uses multi-step observation inputs to capture a comprehensive view of observational data. RT-2 [2] innovates by conceptualizing robot actions as a form of language. Furthermore, RT-H [3] introduces an action hierarchy through language motions, leveraging the chain-of-thought reasoning capabilities of large pre-trained language models. However, while capable of high-level task decomposition, prior models struggle with learning low-level action primitives. Our algorithm addresses this by employing reinforcement learning to master low-level action primitives. Additionally, prior models often lack mechanisms for correcting potential failure cases. Our algorithm addresses this by incorporating sparse failure guidance, thereby strengthening the robustness of our method.

Foundation models significantly enhance robot manipulation capabilities by offering valuable reward signals. CLIP [4], for instance, aligns image representations with language embeddings. Consequently, [10] employs CLIP to measure the reward distance between a robot’s current observation and its linguistic goal. LIV [5] innovatively combines VIP [27] and CLIP to more effectively learn both visual and linguistic goal representations. RoboCLIP [11] adopts the S3D [12] representation model to assess the reward for the final observation of a trajectory. Furthermore, RL-VLM-F [28] directly utilizes GPT-4V to label preferences for agent rollout data.

However, current models still struggle to master a broad spectrum of robot tasks, often succeeding only in simple tasks such as closing a drawer. Vision-language models like CLIP [4] and LIV [5] lack an understanding of the manipulation process. While RoboCLIP [11] offers a sparse reward signal that aids in policy learning, it lacks spatial reasoning capabilities and task completion awareness. RL-VLM-F [28] excels in spatial reasoning for manipulation tasks but is deficient in process understanding capabilities. In contrast, our algorithm not only comprehends detailed language instructions from the robot chain-of-thought but also considers failure scenarios. Additionally, it leverages VLM’s spatial reasoning ability through success experience regularization, offering a more comprehensive approach to mastering robot tasks.

3 Background

We consider scenarios where the robotic system receives specific verbal commands, such as "open the door." To model this learning process, we employ a Markov Decision Process (MDP) defined

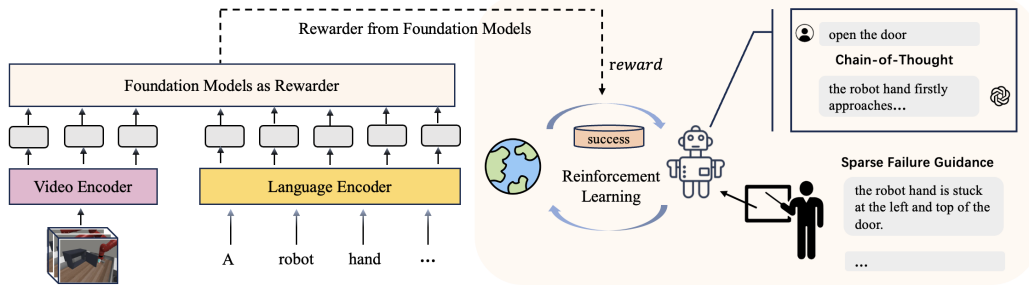


Figure 1: First, the robot receives the language instruction, e.g., "open the door." Subsequently, our algorithm interprets this instruction using the robot chain-of-thought processing, breaking it down into several detailed prompts. The robot also considers some failure guidance. Then, the robot initiates reinforcement learning with our designed reward signal to learn the skills. Successful experiences are recorded by foundation models to reinforce effective behaviors.

by (S, A, r, P, γ) , where S denotes the state space, A the action space, r the reward model, P the transition model, and γ the discount factor.

Chain-of-Thought (CoT) The CoT [29] approach is a reasoning method designed to enhance the problem-solving capabilities of large language models. This method involves decomposing a problem into a series of intermediate steps or thoughts that collectively guide towards a solution, mirroring the human approach to complex problem solving. By explicitly detailing these intermediate steps, large language models such as GPT-4V are better equipped to navigate and resolve complex challenges that require advanced understanding and logical deduction.

VideoCLIP VideoCLIP [30] is a multi-modal model that connects visual and textual information, specifically designed to understand videos by associating them with relevant text descriptions. The model is trained on a diverse dataset of videos and associated texts, allowing it to develop a nuanced understanding of the relationship between video segments and language. In particular, VideoCLIP minimizes the sum of two multi-modal contrastive losses:

$$\mathcal{L} = - \sum_{(v,t) \in \mathcal{B}} (\log \text{NCE}(z_v, z_t) + \log \text{NCE}(z_t, z_v)), \quad (1)$$

where \mathcal{B} is the batch containing sampled video-text pairs, and $\text{NCE}(z_v, z_t)$ and $\text{NCE}(z_t, z_v)$ correspond to the contrastive loss on video-to-text similarity and vice versa. Specifically, the video-to-text contrastive loss is given by:

$$\text{NCE}(z_v, z_t) = \frac{\exp(z_v \cdot z_t^+ / \tau)}{\sum_{z \in \{z_t^+, z_t^-\}} \exp(z_v \cdot z / \tau)}, \quad (2)$$

where τ is a temperature hyper-parameter, z_t^+ and z_t^- are positive and negative text embeddings respectively, and z_v is a video segment embedding.

4 Method

In section 4.1, we introduce the robot chain-of-thought interpretation of the language instruction. In section 4.2, we explain how to define the rewards for policy learning with foundation models. Next, in section 4.3, we discuss policy learning with success experience regularization. Finally, section 4.4 outlines the pipeline of our algorithm.

4.1 Robot Chain-of-Thought

Manipulation skills consist of a series of actionable control steps. For instance, opening a door includes sub-tasks such as approaching the handle, grasping it, pulling it back, and opening the door. Decomposing tasks simplifies the manipulation process, affording robots a greater level of understanding and control.

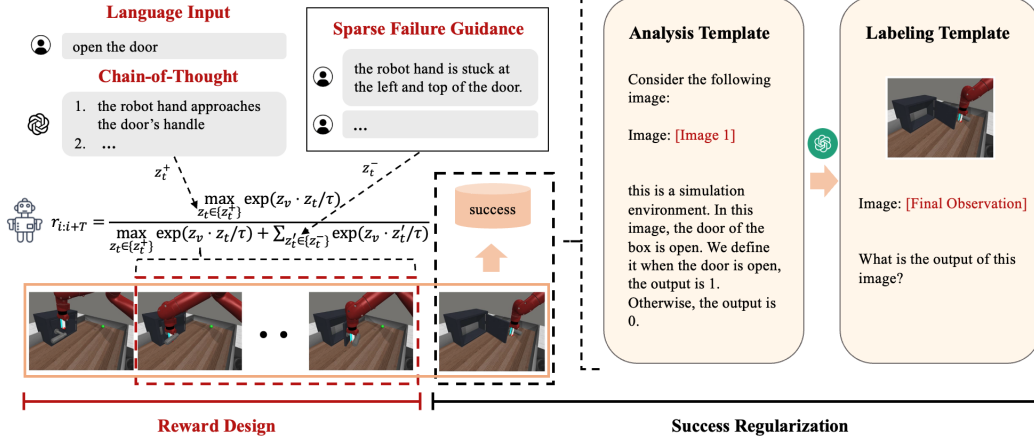


Figure 2: First, text embeddings are generated using robot chain-of-thought (positive prompts) and human failure guidance (negative prompts). Next, a moving window slides across the agent’s rollout trajectory, calculating the NCE reward based on both video and text embeddings. Finally, foundation models evaluate the final observation. If this observation is deemed successful, this trajectory is recorded in the success experience replay buffer for policy regularization.

We use GPT-4V to interpret task instructions such as "open the door." With GPT-4V, this instruction is broken down into a series of sub-goals l_i^+ through a CoT process, such as "the robot hand approaches the door’s handle," "the robot hand grasps the door’s handle," "the robot hand pulls the door’s handle back," and "the robot hand opens the door." Consequently, we leverage the fine-grained task descriptions from GPT-4V interpretation to enhance the agent’s understanding of the tasks.

4.2 Foundation Models as Rewarder

The agent acquires manipulation skills by interacting with an environment, guided by language inputs. A central challenge we address is defining a reward function that effectively reinforces desired behaviors. In this work, we argue that pre-trained vision-language models can provide the agent with prior task knowledge, i.e., how to manipulate objects. Consequently, we propose a novel reward design mechanism based on robot CoT. Specifically, we explore the usage of VideoCLIP [30] as a vision-language foundation model. VideoCLIP excels in capturing the temporal dynamics of video segments and interpreting associated language prompts, aiming to align robot movements with actions described in the task descriptions.

The reward signal for learning manipulation skills is defined as follows:

$$\text{reward} = \frac{\max_{z_l \in \{z_l^+\}} \exp(z_v \cdot z_l / \tau)}{\max_{z_l \in \{z_l^+\}} \exp(z_v \cdot z_l / \tau) + \sum_{z_l' \in \{z_l^-\}} \exp(z_v \cdot z_l' / \tau)}, \quad (3)$$

where z_v is the video segment embedding obtained using a moving window sliding on the agent rollout trajectory, z_l^+ is a set of detailed task description embeddings from robot CoT interpretation l^+ , and z_l^- is a set of potential failure case description embeddings guided by humans. Here, offline human failure guidance helps the agent consider potential failure cases, improving the policy for robustly learning manipulation skills. To enable the agent to recognize and adjust to potential setbacks, we provide sparse human failure guidance before training with 2 to 4 prompts. The training of VideoCLIP, employing a methodology akin to the InfoNCE loss, aims to distinguish between video segments and corresponding positive or negative texts. We argue that a similar NCE-based reward formulation can leverage the VideoCLIP model rather than the reward definition in RoboCLIP [11]. Moreover, the max operation in Equation 3 ensures that robot behaviors aligning with the detailed task descriptions and avoiding failure scenarios yield higher rewards to the agent. Otherwise, the reward signal would penalize undesired behaviors.

4.3 Policy Learning with Success Experience Regularization

Our reward design mechanism motivates the agent to explore the necessary manipulation skills. Empirically, we find that the VideoCLIP rewards don’t reflect the completion of the manipulation tasks well. They focus mostly on whether the robot’s movements align with detailed language goals. To better reinforce task completion, we introduce policy learning with success experience regularization.

We employ GPT-4V to assess the success of the agent’s final observation in its rollout trajectory. If it is deemed successful, this trajectory is archived into a success experience replay buffer and we correct the reward function as: $r(s_T) = r(s_T) + 100$. Here, s_T is the successful final observation of the rollout trajectory. Subsequently, we introduce a regularization mechanism aimed at refining the agent’s policy to reinforce successful behavior. This motivates the agent to reinforce the success experience. The regularization loss is integrated with the policy loss, formulated as follows:

$$\mathcal{L} = \text{RL Loss} + \lambda \sum_{(s,a) \in D_E} -\log(\pi(a|s)), \quad (4)$$

where D_E is the success experience replay buffer and λ is the hyper-parameter. By incorporating success experiences into the policy loss calculation, the agent is encouraged to repeat desired behaviors.

4.4 Pipeline

Our algorithm begins with GPT-4V interpreting language instructions into detailed task descriptions. Meanwhile, humans guide the agent with several potential failure case descriptions. Subsequently, rewards are calculated following Equation 3 with a moving window that slides over the agent’s rollout trajectories. The agent is then updated with these learned rewards through reinforcement learning. Concurrently, GPT-4V evaluates the final observation of the rollout trajectory and assigns a success label, indicating whether it is a successful observation. If it is successful, we record the trajectory into a success experience replay buffer for policy regularization and correct the reward of final observation with $r(s_T) = r(s_T) + 100$.

Figure 2 illustrates our method for computing rewards and success regularization that aid the robot in learning manipulation skills. This involves a moving window that traverses the agent’s rollout trajectory, the computation of NCE rewards using language prompts, and the policy regularization using success experiences gathered through GPT-4V. This comprehensive approach aims to effectively teach the agent desired manipulation skills through reinforcement learning.

5 Experiment

In this section, we assess the effectiveness of our proposed algorithm by conducting experiments in comparison with several baseline models. The experiments are designed to address two questions: (1) How does our algorithm perform compared to other state-of-the-art algorithms? The results are presented in section 5.1. (2) What are the contributing factors in our algorithm? The ablation studies are presented in section 5.2.

Environments To evaluate the effectiveness of our proposed algorithm, we conduct experiments on a wide array of manipulation tasks using MetaWorld-v2 as the test robotic environment. We select 10 tasks from simple to complex, including drawer, window, faucet, button press, door, and soccer, as described by [31]. Among these tasks, opening objects such as drawers, windows, faucets, and doors is significantly more challenging than closing them.

Setup To ensure a fair evaluation across all experiments, we use DrQ-v2 [32] as the reinforcement learning algorithm. Detailed implementation specifics can be found in the references: CLIP [10], LIV [5], and RoboCLIP [11]. All experiments, including those involving our proposed algorithm, receive the same language instructions as inputs. Implementation details are provided in the Appendix.

5.1 Overall Comparison

To demonstrate the superiority of our algorithm, we conduct a series of experiments comparing it with established baselines: CLIP [10], LIV [5], and RoboCLIP [11]. CLIP (as described in [10])

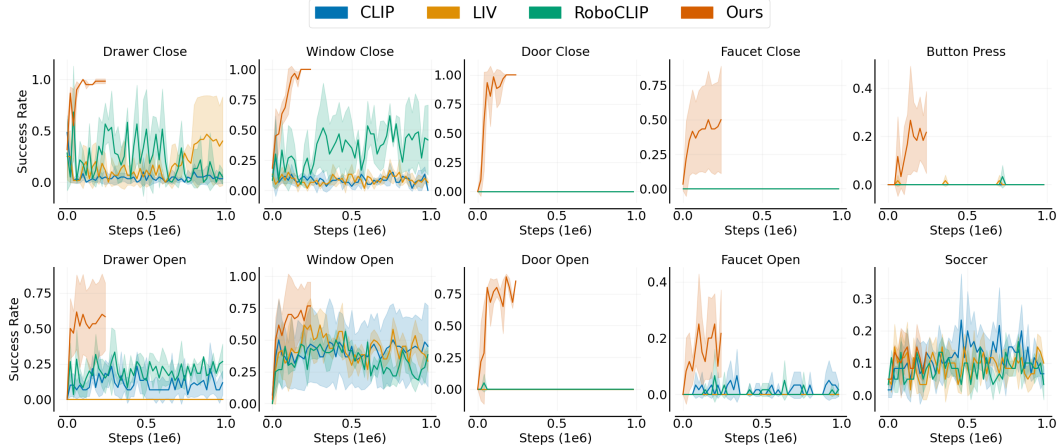


Figure 3: Training curves for baselines and our algorithm within 3 random seeds. Each data point is evaluated with 20 sampled trajectories. The shaded area displays the range of one standard deviation. Our algorithm gets best performance compared to other baselines, achieves $5.4\times$ improvement compared to RoboCLIP.

employs CLIP [4] as the vision-language model to measure the distance between current observations and language goals. LIV [5] aligns goal representations with language instructions, and RoboCLIP [11] utilizes S3D [12] to measure the distance between trajectory videos and language as a form of reward. However, CLIP [4] and LIV [5] lack an understanding of the manipulation process, while RoboCLIP [11] lacks spatial reasoning capabilities and task completion awareness. Figure 3 illustrates the training curves, depicting the success rates for each algorithm. Each evaluation involves 20 trajectories, and the experiments were replicated across three different environmental random seeds to introduce variability in the position of objects.

Our findings indicate distinct performance trends across various tasks. RoboCLIP displays promising results in tasks involving drawer and window manipulation, as well as soccer, but it is most effective in the simplest tasks such as drawer closing. CLIP performs well in tasks related to faucet, drawer and window manipulation, and soccer, indicating that CLIP focuses more on task completion rather than the manipulation process. LIV shows competence primarily in tasks involving drawer closure, window opening, and soccer. Our algorithm consistently outperforms the baselines across all tasks, achieving success rates exceeding 75% in tasks such as closing and opening drawers, windows, and doors. These results underscore the effectiveness of our approach in handling diverse and challenging scenarios.

5.2 Ablation Study

In this section, we conduct ablation studies by removing each component of our algorithm (CoT interpretation, human failure guidance, and success regularization). The results indicate that the most contributing factor to our algorithm’s performance is success regularization, followed by human failure guidance. Each component contributes to the overall performance of our algorithm. Additionally, we conduct ablation studies comparing GPT-4V success labels with ground truth success labels, demonstrating the robustness of our GPT-4V labeling. Furthermore, we explore different reward design mechanisms, showing that they can also achieve high performance within our algorithm. Finally, experiments with all baselines incorporating success regularization reveal that our algorithm’s superiority is not solely due to success regularization but also the reward design mechanism.

Question 1: how significant is each component of our algorithm in contributing to the results?

Our algorithm incorporates several critical components: robot chain-of-thought processing via GPT-4V, sparse human failure guidance, and success experience regularization. To evaluate the significance of each component, we conducted a series of experiments, systematically removing each component

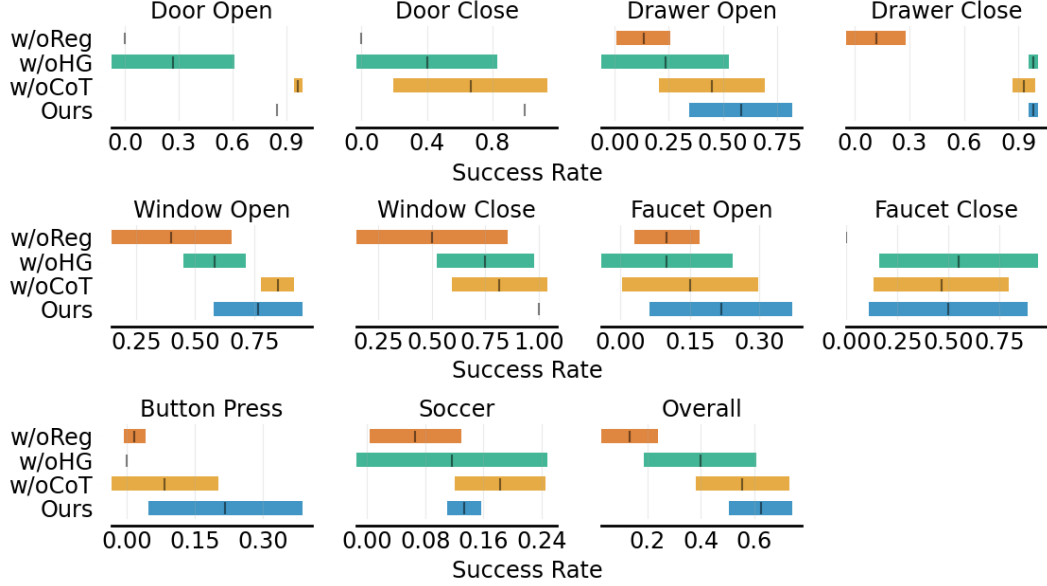


Figure 4: Final policy performance for ablations and our algorithm across 3 random seeds. The results show that success regularization is the most significant contributing factor in our algorithm, followed by human failure guidance. Each component contributes to the overall performance of our algorithm.

to observe its impact on performance. A decline in performance upon the removal of any component demonstrates its essential role in our algorithm.

Figure 4 illustrates the success rates of the final policy performance of our algorithm compared to its ablated versions. The labels for these ablations are: w/oReg (without success experience regularization), w/oHG (without sparse human failure guidance), and w/oCoT (without robot chain-of-thought task decomposition).

The results confirm the critical importance of each component in our algorithm, with success experience regularization being particularly pivotal. Human failure guidance is the second most important component, motivating the agent to consider potential failure cases. Additionally, robot chain-of-thought processing helps the agent better understand the process of manipulation tasks, further contributing to the performance of our algorithm.

Question 2: what is the empirical difference between the labels assigned by GPT-4V and the ground truth labels in the context of success experience collection?

Our algorithm incorporates GPT-4V to gather successful trajectories for policy regularization. To validate the robustness of our GPT-4V labeling in collecting success experiences, we conduct experiments comparing GPT-4V labels and ground truth labels. If the performance using GPT-4V labels is similar to that using ground truth labels, it would confirm that GPT-4V is robust in collecting success experiences.

The process for GPT-4V analysis is outlined in Figure 2. Initially, we present GPT-4V with a scenario indicating a successful state (e.g., the door is open). We then provide a prompt: "Consider the following image; this is a simulation environment. In this image, the door of the box is open. We define it when the door is open, the output is 1. Otherwise, the output is 0." Subsequently, we present the final observation to GPT-4V and prompt, "What is the output of this image?" We collect the trajectory as successful when GPT-4V's response is 1.

Figure 5 displays the training success rate curves comparing GPT-4V and ground truth (GT) labeling methods for success experience collection. Our findings show that the GPT-4V labeling method achieves performance comparable to the ground truth across various tasks, demonstrating the robustness of our GPT-4V success labels.

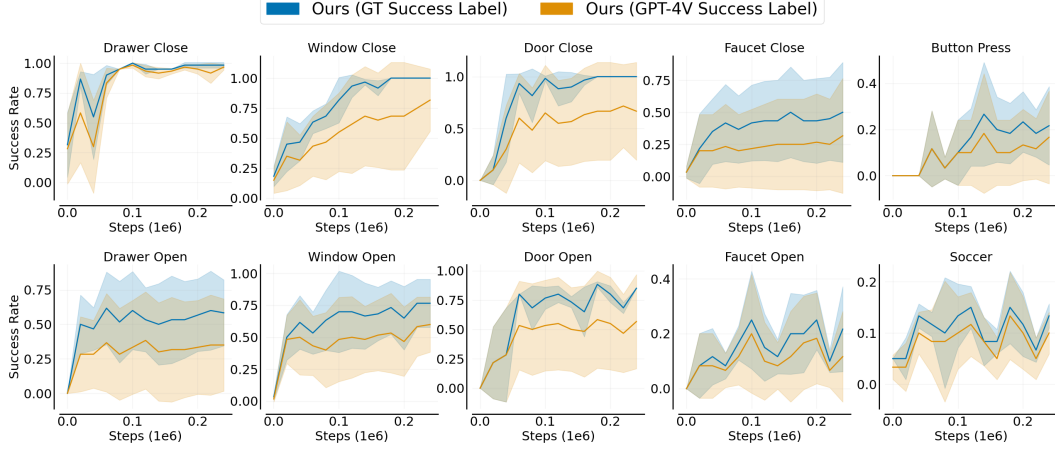


Figure 5: Ablation study for our algorithm with different success labeling methods (GPT-4V labeling or ground truth (GT) labeling). The results demonstrate that the success labels generated by GPT-4V are robust.

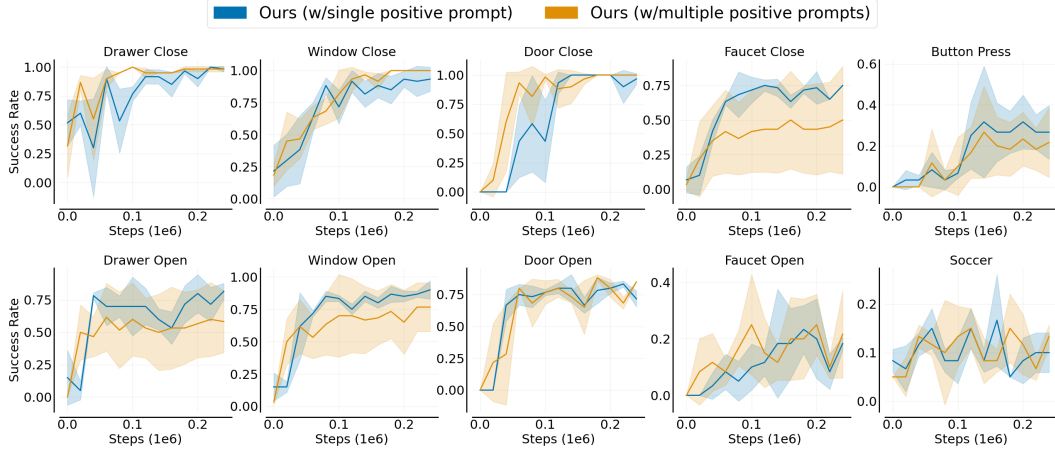


Figure 6: Ablation study for our algorithm with CoT as one single prompt or multiple prompts. The results show that single prompt for reward mechanism also works well.

Question 3: what is the empirical difference between our algorithm and the one with a single chain-of-thought interpreted positive prompt?

Our algorithm computes the NCE-rewards based on the maximum distance between the moving window video and multiple positive prompts. This measurement indicates how far the moving window video is from the language goal derived from robot chain-of-thought interpretations. Conversely, our ablation method computes the NCE-rewards based on the distance between the moving window video and a single interpreted positive prompt. The NCE-reward function is shown as:

$$\text{reward} = \frac{\exp(z_v \cdot z_l^+ / \tau)}{\exp(z_v \cdot z_l^+ / \tau) + \sum_{z_l' \in \{z_l^-\}} \exp(z_v \cdot z_l' / \tau)}, \quad (5)$$

where z_l^+ indicates the single positive prompt from the GPT-4V interpretation. For example, the prompt for opening a door is "the robot hand first approaches the door's handle, then grasps it, pulls it back, and finally opens the door."

Figure 6 shows the comparison between our algorithm with multiple positive prompts and the single positive prompt ablation. The empirical results demonstrate that our algorithm achieves comparable results with a single positive prompt. It indicates that our algorithm is robust to the setting of multiple or single positive prompts.

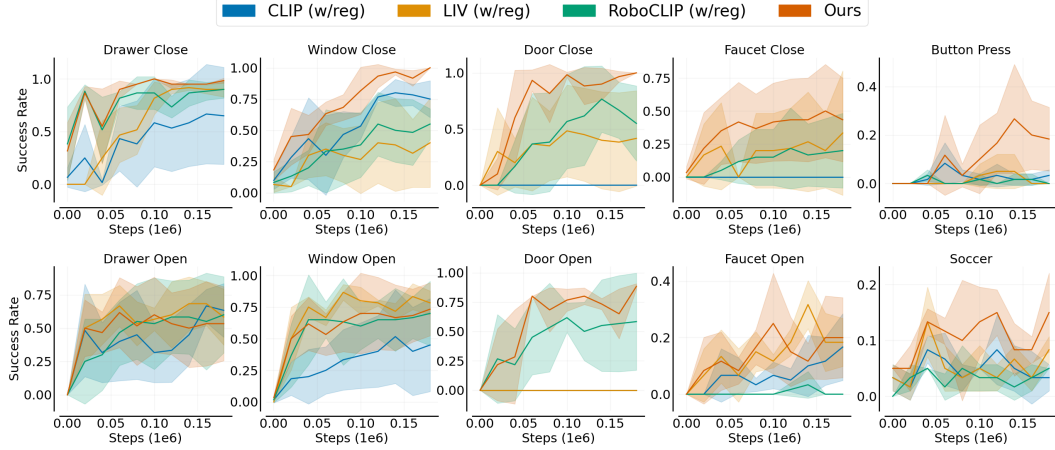


Figure 7: Ablation study for all baselines with success experience regularization. The results show that our algorithm performs well not only because of the success regularization component but also due to the reward design mechanism.

Question 4: what is the empirical difference between our algorithm and all baselines with success experience regularization?

Question 1 shows that success experience regularization component plays the most important role in our algorithm. To evaluate the significance of the reward design mechanism, we conduct experiments applying success regularization to all baselines. If the results show that our algorithm still outperforms other baselines with success regularization, then it proves that our algorithm’s superiority is due not only to the success regularization but also to the reward design mechanism.

Figure 7 shows the ablation results comparing our algorithm with other state-of-the-art baselines that include success experience regularization. The results demonstrate that our algorithm outperforms other baselines on almost all tasks. This indicates that our algorithm’s superiority is due not only to the success regularization component but also to the reward design mechanism.

6 Conclusion

In this study, we present a novel algorithm for robotic manipulation skill acquisition. We propose that pre-trained vision-language models can instruct robots on prior knowledge essential for manipulation tasks. Our algorithm simplifies complex tasks and acquires manipulation skills through a robot’s chain-of-thought process with sparse failure guidance, mirroring the developmental learning trajectory of a child. Specifically, our algorithm is designed to extract intricate temporal visual cues from the robot’s thought process, enabling a nuanced understanding of the task at hand. It also incorporates a learning strategy by describing potential failure cases through sparse failure guidance, which enhances its manipulation policies. Through success experience regularization, our algorithm strengthens its policies, thereby improving performance. Empirical results confirm the effectiveness of our approach, demonstrating a distinct advantage over established baseline models. This research sets a new standard for mastering manipulation skills in robots, and we hope it can be applied to more robotic manipulation tasks in the future.

References

- [1] Anthony Brohan, Noah Brown, Justice Carbajal, Yevgen Chebotar, Joseph Dabis, Chelsea Finn, Keerthana Gopalakrishnan, Karol Hausman, Alex Herzog, Jasmine Hsu, et al. Rt-1: Robotics transformer for real-world control at scale. *arXiv preprint arXiv:2212.06817*, 2022.
- [2] Anthony Brohan, Noah Brown, Justice Carbajal, Yevgen Chebotar, Xi Chen, Krzysztof Choromanski, Tianli Ding, Danny Driess, Avinava Dubey, Chelsea Finn, et al. Rt-2: Vision-language-

- action models transfer web knowledge to robotic control. *arXiv preprint arXiv:2307.15818*, 2023.
- [3] Suneel Belkale, Tianli Ding, Ted Xiao, Pierre Sermanet, Quon Vuong, Jonathan Tompson, Yevgen Chebotar, Debidatta Dwibedi, and Dorsa Sadigh. Rt-h: Action hierarchies using language. *arXiv preprint arXiv:2403.01823*, 2024.
 - [4] Alec Radford, Jong Wook Kim, Chris Hallacy, Aditya Ramesh, Gabriel Goh, Sandhini Agarwal, Girish Sastry, Amanda Askell, Pamela Mishkin, Jack Clark, et al. Learning transferable visual models from natural language supervision. In *International conference on machine learning (ICML)*, pages 8748–8763. PMLR, 2021.
 - [5] Yecheng Jason Ma, Vikash Kumar, Amy Zhang, Osbert Bastani, and Dinesh Jayaraman. Liv: Language-image representations and rewards for robotic control. In *International Conference on Machine Learning (ICML)*, pages 23301–23320. PMLR, 2023.
 - [6] Jean-Baptiste Alayrac, Jeff Donahue, Pauline Luc, Antoine Miech, Iain Barr, Yana Hasson, Karel Lenc, Arthur Mensch, Katherine Millican, Malcolm Reynolds, et al. Flamingo: a visual language model for few-shot learning. *Advances in neural information processing systems (NeurIPS)*, 35:23716–23736, 2022.
 - [7] Adrienne Wright, Yuting Zhao, and Martin Ivanov. Palm: Scaling language modeling with pathways.
 - [8] Xinghang Li, Minghuan Liu, Hanbo Zhang, Cunjun Yu, Jie Xu, Hongtao Wu, Chilam Cheang, Ya Jing, Weinan Zhang, Huaping Liu, et al. Vision-language foundation models as effective robot imitators. *International Conference on Learning Representations (ICLR)*, 2024.
 - [9] Danny Driess, Fei Xia, Mehdi SM Sajjadi, Corey Lynch, Aakanksha Chowdhery, Brian Ichter, Ayzan Wahid, Jonathan Tompson, Quan Vuong, Tianhe Yu, et al. Palm-e: An embodied multimodal language model. *arXiv preprint arXiv:2303.03378*, 2023.
 - [10] Juan Rocamonde, Victoriano Montesinos, Elvis Nava, Ethan Perez, and David Lindner. Vision-language models are zero-shot reward models for reinforcement learning. *arXiv preprint arXiv:2310.12921*, 2023.
 - [11] Sumedh Anand Sontakke, Jesse Zhang, Séb Arnold, Karl Pertsch, Erdem Biyik, Dorsa Sadigh, Chelsea Finn, and Laurent Itti. RoboCLIP: One demonstration is enough to learn robot policies. In *Thirty-seventh Conference on Neural Information Processing Systems (NeurIPS)*, 2023.
 - [12] Saining Xie, Chen Sun, Jonathan Huang, Zhuowen Tu, and Kevin Murphy. Rethinking spatiotemporal feature learning: Speed-accuracy trade-offs in video classification. In *Proceedings of the European conference on computer vision (ECCV)*, pages 305–321, 2018.
 - [13] Mohit Shridhar, Lucas Manuelli, and Dieter Fox. Perceiver-actor: A multi-task transformer for robotic manipulation. In *Conference on Robot Learning (CoRL)*, pages 785–799. PMLR, 2023.
 - [14] Mohit Shridhar, Lucas Manuelli, and Dieter Fox. Cliport: What and where pathways for robotic manipulation. In *Conference on robot learning (CoRL)*, pages 894–906. PMLR, 2022.
 - [15] Octo Model Team, Dibya Ghosh, Homer Walke, Karl Pertsch, Kevin Black, Oier Mees, Sudeep Dasari, Joey Hejna, Charles Xu, Jianlan Luo, et al. Octo: An open-source generalist robot policy, 2023.
 - [16] Jonathan Ho and Stefano Ermon. Generative adversarial imitation learning. *Advances in neural information processing systems (NeurIPS)*, 29, 2016.
 - [17] Yuyang Liu, Weijun Dong, Yingdong Hu, Chuan Wen, Zhao-Heng Yin, Chongjie Zhang, and Yang Gao. Imitation learning from observation with automatic discount scheduling. *International Conference on Learning Representations (ICLR)*, 2024.
 - [18] Stéphane Ross, Geoffrey Gordon, and Drew Bagnell. A reduction of imitation learning and structured prediction to no-regret online learning. In *Proceedings of the fourteenth international conference on artificial intelligence and statistics (AISTATS)*, pages 627–635. JMLR Workshop and Conference Proceedings, 2011.

- [19] Chuan Wen, Jierui Lin, Trevor Darrell, Dinesh Jayaraman, and Yang Gao. Fighting copycat agents in behavioral cloning from observation histories. *Advances in Neural Information Processing Systems (NeurIPS)*, 33:2564–2575, 2020.
- [20] Chuan Wen, Jianing Qian, Jierui Lin, Dinesh Jayaraman, and Yang Gao. Fight fire with fire: countering bad shortcuts in imitation learning with good shortcuts. *International Conference on Machine Learning (ICML)*, 2022.
- [21] Rae Jeong, Yusuf Aytar, David Khosid, Yuxiang Zhou, Jackie Kay, Thomas Lampe, Konstantinos Bousmalis, and Francesco Nori. Self-supervised sim-to-real adaptation for visual robotic manipulation. In *2020 IEEE international conference on robotics and automation (ICRA)*, pages 2718–2724. IEEE, 2020.
- [22] Jan Matas, Stephen James, and Andrew J Davison. Sim-to-real reinforcement learning for deformable object manipulation. In *Conference on Robot Learning (CoRL)*, pages 734–743. PMLR, 2018.
- [23] Zhenjia Xu, Zhou Xian, Xingyu Lin, Cheng Chi, Zhiao Huang, Chuang Gan, and Shuran Song. Roboninja: Learning an adaptive cutting policy for multi-material objects. *arXiv preprint arXiv:2302.11553*, 2023.
- [24] Michael Ahn, Anthony Brohan, Noah Brown, Yevgen Chebotar, Omar Cortes, Byron David, Chelsea Finn, Chuyuan Fu, Keerthana Gopalakrishnan, Karol Hausman, et al. Do as i can, not as i say: Grounding language in robotic affordances. *arXiv preprint arXiv:2204.01691*, 2022.
- [25] Suraj Nair, Aravind Rajeswaran, Vikash Kumar, Chelsea Finn, and Abhinav Gupta. R3m: A universal visual representation for robot manipulation. *Conference on Robot Learning (CoRL)*, 2022.
- [26] Pierre Sermanet, Corey Lynch, Yevgen Chebotar, Jasmine Hsu, Eric Jang, Stefan Schaal, Sergey Levine, and Google Brain. Time-contrastive networks: Self-supervised learning from video. In *2018 IEEE international conference on robotics and automation (ICRA)*, pages 1134–1141. IEEE, 2018.
- [27] Yecheng Jason Ma, Shagun Sodhani, Dinesh Jayaraman, Osbert Bastani, Vikash Kumar, and Amy Zhang. Vip: Towards universal visual reward and representation via value-implicit pre-training. *International Conference on Learning Representations (ICLR)*, 2023.
- [28] Yufei Wang, Zhanyi Sun, Jesse Zhang, Zhou Xian, Erdem Biyik, David Held, and Zackory Erickson. RL-vlm-f: Reinforcement learning from vision language foundation model feedback. *arXiv preprint arXiv:2402.03681*, 2024.
- [29] Jason Wei, Xuezhi Wang, Dale Schuurmans, Maarten Bosma, Fei Xia, Ed Chi, Quoc V Le, Denny Zhou, et al. Chain-of-thought prompting elicits reasoning in large language models. *Advances in neural information processing systems (NeurIPS)*, 35:24824–24837, 2022.
- [30] Hu Xu, Gargi Ghosh, Po-Yao Huang, Dmytro Okhonko, Armen Aghajanyan, Florian Metze, Luke Zettlemoyer, and Christoph Feichtenhofer. Videoclip: Contrastive pre-training for zero-shot video-text understanding. *Conference on Empirical Methods in Natural Language Processing (EMNLP)*, 2021.
- [31] Siddhant Halder, Vaibhav Mathur, Denis Yarats, and Lerrel Pinto. Watch and match: Supercharging imitation with regularized optimal transport. In *Conference on Robot Learning*, pages 32–43. PMLR, 2023.
- [32] Denis Yarats, Rob Fergus, Alessandro Lazaric, and Lerrel Pinto. Mastering visual continuous control: Improved data-augmented reinforcement learning. *arXiv preprint arXiv:2107.09645*, 2021.

7 Appendix

7.1 Environment Setup

We use MetaWorld-v2 as our test robotic environments. We choose 10 tasks as by [31] to evaluate our algorithm and baselines. They are drawer close, window close, door close, faucet close, button press, drawer open, window open, door open, faucet open and soccer. Among these tasks, opening objects such as drawers, windows, faucets, and doors is significantly more challenging than closing them.

To reduce the exploration space, we set the gripper a new position. With varying random seeds, the objects like drawer, window, door, faucet, button, and soccer would vary its positions. The position coordinate are provided in Table 1.

Table 1: Position coordinates for robot gripper as setting with MetaWorld-v2.

TASK	COORDINATE
DRAWER CLOSE	0, 0.6, 0.2
DRAWER OPEN	0, 0.8, 0.05
WINDOW CLOSE	0.25, 0.80, 0.16
WINDOW OPEN	-0.15, 0.77, 0.16
DOOR CLOSE	-0.5, 0.6, 0.2
DOOR OPEN	0, 0.6, 0.2
FAUCET CLOSE	0., 0.6, 0.1
FAUCET OPEN	0., 0.6, 0.1
BUTTON PRESS	0, 0.6, 0.2
SOCCER	0., 0.6, 0.06

Since the default camera view is not suitable for our algorithms. We re-set the camera for training all the experiments. The principle for choosing camera is that we set the object and gripper in the view. The camera coordinates are provided in Table 2.

Table 2: Position coordinates and angles for camera as setting with MetaWorld-v2.

TASK	COORDINATE	ANGLE
DOOR CLOSE	-1.1, -0.4, 0.6	-
OTHER TASKS	0.55, 0.3, 0.5	3.9, 2.3, 0.6

7.2 GPT-4V Success Labeling Details

Our algorithm incorporates GPT-4V to gather successful trajectories for policy regularization. The process for GPT-4V analysis is outlined in Figure 8. Initially, we present GPT-4V with a scenario indicating a successful state (e.g., the door is open). We then provide a prompt: "Consider the following image; this is a simulation environment. In this image, the door of the box is open. We define it when the door is open, the output is 1. Otherwise, the output is 0." Subsequently, we present the final observation to GPT-4V and prompt, "What is the output of this image?" We collect the trajectory as successful when GPT-4V's response is 1.

To reduce the query times with GPT-4V, we distill a classifier from GPT-4V labeling data. First, we use GPT-4V to label 300 pictures with diverse final observations. Next, we fine-tune a ResNet-18 classifier based on this dataset. Before training, we use some augmentation techniques such as random crop resize to augment the dataset. Finally, we use this classifier to classify the final observation as successful or not for instance.

7.3 Task Robot Chain-of-Thought Prompt

Manipulation skills consist of a series of actionable control steps. For instance, opening a door includes sub-tasks such as approaching the handle, grasping it, pulling it back, and opening the

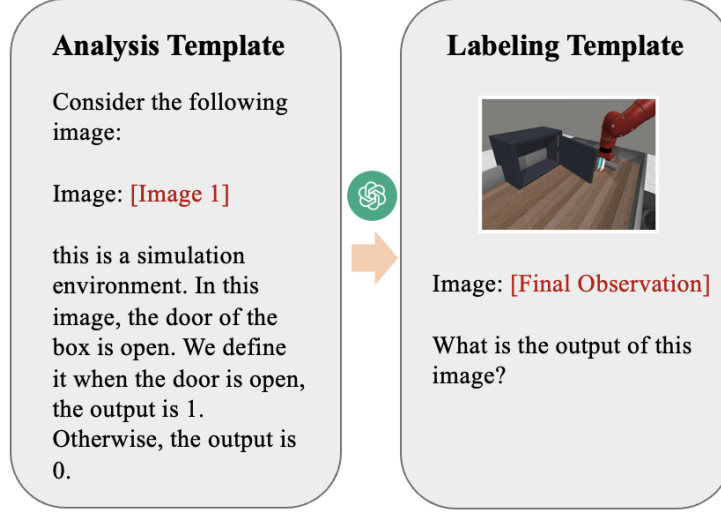


Figure 8: The successful trajectories are gathered through GPT-4V success labeling. GPT-4V would label the success preference to the final observation of agent’s rollout trajectory. If it deemed successful, the trajectory would be recorded into a replay buffer.

door. Decomposing tasks simplifies the manipulation process, affording robots a greater level of understanding and control.

We use GPT-4V to interpret task instructions such as "open the door." With GPT-4V, this instruction is broken down into a series of sub-goals z_l^+ through a CoT process, such as "the robot hand approaches the door’s handle," "the robot hand grasps the door’s handle," "the robot hand pulls the door’s handle back," and "the robot hand opens the door." Consequently, we leverage the fine-grained task descriptions from GPT-4V interpretation to enhance the agent’s understanding of the tasks. The task robot CoT prompts are provided in Table 3.

7.4 Sparse Human Failure Guidance

Robots may encounter potential failures during learning. Offline human failure guidance helps the agent consider potential failure cases, improving the policy for robustly learning manipulation skills.

z_l^- is a set of offline potential failure case descriptions consisting of 2 to 4 prompts. To enable the agent to recognize and adjust to potential failures, we provide sparse human failure guidance before training the agent. The sparse human failure guidance are provided in Table 4.

Table 3: Prompts from robot chain-of-thought for task interpretation.

Task	Robot Chain-of-Thought Prompts
Drawer Close	the robot hand pushes the drawer; the drawer is closed.
Drawer Open	the robot hand moves to the top of the drawer’s handle; the robot hand moves inside the drawer’s handle; the robot hand pulls back the drawer’s handle; the robot hand opens the drawer.
Window Close	the robot hand moves to the left of the window’s handle; the robot hand pushes the handle towards right; the robot hand closes the window.
Window Open	the robot hand moves to the right of the window’s handle; the robot hand pushes the handle towards left; the robot hand opens the window.
Door Close	the robot hand pushes the door close; the door is closed.
Door Open	the robot hand is at the front of the door; the robot hand moves to the left of the door’s handle; the robot hand pulls back the door’s handle; the robot hand opens the door
Faucet Close	the robot hand moves to the left of the faucet; the robot hand pulls the faucet towards right; the faucet is closed.
Faucet Open	the robot hand moves to the right of the faucet; the robot hand pulls the faucet towards left; the faucet is open.
Button Press	the robot hand moves towards the red button; the robot hand pushes the button; the button is pressed.
Soccer	the robot hand moves towards soccer; the robot hand pushes soccer into the net; the soccer is in the net.

Table 4: Sparse human failure guidance.

Task	Human Failure Guidance
Drawer Close	the robot hand is moving away from the drawer; the robot hand is at the left of the drawer; the robot hand is at the right of the drawer.
Drawer Open	the robot hand is at the right of the drawer’s handle; the robot hand is at the left of the drawer’s handle; the robot hand is under the drawer’s handle.
Window Close	the robot hand is at the top of the window’s handle; the robot hand is at the right of the window’s handle; the robot hand is under the window’s handle.
Window Open	the robot hand is at the top of the window’s handle; the robot hand is at the left of the window’s handle; the robot hand is under the window’s handle.
Door Close	the robot hand is moving away from the door; the robot hand is at the left of the door.
Door Open	the robot hand is at the right of the door’s handle; the robot hand is at the top of the door’s handle; the robot hand is under the door’s handle; the robot hand is at the left of the box.
Faucet Close	the robot hand is to the right of the faucet; the robot hand is at the top of the faucet.
Faucet Open	the robot hand is to the left of the faucet; the robot hand is at the top of the faucet.
Button Press	the robot hand moves away from the red button; the robot hand is at the left of the red button; the robot hand is at the right of the red button.
Soccer	the robot hand is moving away from soccer; the robot hand is at the top of soccer.